Author Manuscript

Author Manuscript

Author Manuscript

Author Manuscript

HHS Public Access

Author manuscript

Int J Radiat Oncol Biol Phys. Author manuscript; available in PMC 2019 June 01.

Published in final edited form as:

Int J Radiat Oncol Biol Phys. 2018 June 01; 101(2): 479–489. doi:10.1016/j.ijrobp.2018.02.009.

Impact of spot size and spacing on the quality of robustly-optimized intensity-modulated proton therapy plans for lung cancer

Chenbin Liu, PhD[1], **Steven E. Schild, MD**[1], **Joe Y. Chang, PhD MD**[2], **Zhongxing Liao, MD**[2], **Shawn Korte, CMD**[1], **Jiajian Shen, PhD**[1], **Xiaoning Ding, PhD**[1], **Yanle Hu, PhD**[1], **Yixiu Kang, PhD**[1], **Sameer R. Keole, MD**[1], **Terence T. Sio, MD MS**[1], **William W. Wong, MD**[1], **Narayan Sahoo, PhD**[3], **Martin Bues, PhD**[1], and **Wei Liu, PhD**[1]

[1]Department of Radiation Oncology, Mayo Clinic Arizona, Phoenix, Arizona

[2]Department of Radiation Oncology, The University of Texas MD Anderson Cancer Center, Houston, Texas

[3]Department of Radiation Physics, The University of Texas MD Anderson Cancer Center, Houston, Texas

Abstract

Background—To investigate how spot size and spacing affect plan quality, robustness and interplay effects of robustly optimized intensity-modulated proton therapy (IMPT) for lung cancer.

Methods—Two robustly optimized IMPT plans were created for 10 lung cancer patients: first by a large-spot machine with in-air energy dependent large spot size at isocenter (σ: 6–15 mm) and spacing (1.3σ), and second by a small-spot machine with in-air energy dependent small spot size (σ: 2–6 mm) and spacing (5 mm). Both plans were generated by optimizing radiation dose to internal target volume on averaged 4D-CTs using an in-house developed IMPT planning system. The dose-volume-histograms (DVH) band method was used to evaluate plan robustness. Dose evaluation software was developed to model time-dependent spot delivery to incorporate interplay effects with randomized starting phases for each field per fraction. Patient anatomy voxels were mapped phase-to-phase via deformable image registration (DIR), and doses were scored using in-house developed software. DVH indices including ITV dose coverage, homogeneity, and organs-at-risk (OARs) sparing were compared using Wilcoxon signed-rank test.

Results—Compared to large-spot machine, small-spot machine resulted in significantly lower heart and esophagus mean doses with comparable target dose coverage, homogeneity, and protection of other OARs. Plan robustness was comparable for targets and most OARs. With

Corresponding author: Wei Liu, PhD, Department of Radiation Oncology, Mayo Clinic Arizona, 5777 E. Mayo Boulevard, Phoenix, AZ 85054; Liu.Wei@mayo.edu, Phone:480-342-1262.

Publisher's Disclaimer: This is a PDF file of an unedited manuscript that has been accepted for publication. As a service to our customers we are providing this early version of the manuscript. The manuscript will undergo copyediting, typesetting, and review of the resulting proof before it is published in its final citable form. Please note that during the production process errors may be discovered which could affect the content, and all legal disclaimers that apply to the journal pertain.

Conflicts of Interest Notification

None

Author Manuscript Author Manuscript Author Manuscript Author Manuscript

interplay effects considered, significantly lower heart and esophagus mean doses with comparable target dose coverage and homogeneity were observed using smaller spots.

Conclusions—Robust optimization with small spot-machine significantly improves heart and esophagus sparing with comparable plan robustness and interplay effects compared with robust optimization with large-spot machine. Small-spot machine utilizes a larger number of spots to cover the same tumors compared to large-spot machine, which gives the planning system more freedom to compensate for the higher sensitivity to uncertainties and interplay effects for lung cancer treatments.

Keywords

intensity-modulated proton therapy; spot size; lung cancer; respiratory motion; robust optimization; 4D treatment planning; interplay effects

INTRODUCTION

Lung cancer is the leading cause of cancer death in United States (1). Intensity-modulated proton therapy (IMPT) holds great promise for improving outcomes in lung cancer patients compared to intensity-modulated x-ray therapy (IMRT) and passive scattering proton therapy (PSPT) (2–4).

Unfortunately IMPT is especially vulnerable to patient setup and range uncertainties due to heterogeneous tissues in lung cancer (5, 6). Patient setup and proton range uncertainties can be effectively addressed by robust optimization (3, 7–13), however, respiratory motion in lung cancer treatment may result in range estimate mismatch and thus diminish the effectiveness of robust optimization (14). In addition, beamlet delivery is time-dependent, which may interfere with respiratory motion (typically referred to “interplay effects”). Interplay effects may severely perturb the resulting dose distribution (15–26). Many efforts have been made to minimize this effect, such as range-adapted internal target volume (ITV) (27–29), breath hold (30), gating (31–33), tumor tracking (34, 35), repainting (36–44), and 4D treatment planning (45–49). Some studies have shown that the geometric and radiologic variation due to respiratory motion have limited dosimetric impacts on target coverage and target dose homogeneity of the robustly optimized IMPT plans in lung cancer treatments (14, 50) if the motion amplitude is small.

Spot size and spacing are reported to have significant influence on plan robustness and interplay effects in IMPT for lung cancer (3, 21, 22, 39, 51). It is generally believed that IMPT plans for a proton machine with smaller spots are less robust and suffer more severe impact from interplay effects when treating moving targets. Additionally, smaller spot spacing makes plans less susceptible to interplay effects and improves the target dose homogeneity (21, 22, 39). However, the above conclusions are based on data from non-robustly optimized IMPT plans. As a result, a detailed study was proposed by our group to study the impact of spot size and spacing using robustly optimized IMPT plans for lung cancer treatments.

Author Manuscript Author Manuscript Author Manuscript Author Manuscript

Large spot sizes are common in the first generation of spot scanning proton machines. However, the newly built proton centers over past few years are equipped with small spot size proton machines, which require smaller spot spacing to minimize possible dose ripples and achieve uniform dose distribution within target volumes. Therefore, effective strategies are needed to mitigate interplay effects for the newer spot scanning proton machines, which are common with small spots for lung cancer treatment. The aims of this study are: (1) to study the impact of spot size and spacing in robust IMPT optimization; (2) to investigate whether interplay effects can be effectively mitigated by robust optimization for small spot proton machines.

METHODS AND MATERIALS

Patient Data and Treatment Planning

We retrospectively selected 10 patients with non–small cell lung cancer (NSCLC) and re-planed them using IMPT at two operational proton centers: (1) for a machine (hereafter called large-spot machine) with in-air energy dependent large spot at isocenter (σ: 5–15 mm) and spacing (1.3σ); (2) for a machine (hereafter called small-spot machine) with in-air energy dependent small spot (σ: 2–6 mm) and spacing (fixed at 5 mm). The fixed spot spacing of 5mm used in the small-spot machine was determined during our treatment planning system (TPS) commissioning after careful study by adjusting spot spacing of different proton energies to balance between the requirement to achieve an as uniform as possible target dose distribution in different disease sites and the requirement to minimize the impact of the minimum Monitor Unit (MU) constraints (52). The detailed discussion of this point is beyond the scope of this study and will be included in a manuscript about our TPS commissioning.

The irradiation targets were conventionally defined. The internal gross target volume (IGTV) was formed to encompass the extent of GTV motion in all phases using 4D CT; and then an internal clinical target volume (ICTV), or internal target volume (ITV), was formed by expansion of IGTV by a margin of 8 mm. A representative group of cases were selected to represent varying tumor stages, tumor volumes, and respiratory motion patterns (Table 1). The GTV mass center-to-center motion was used to define the respiratory motion amplitude (RMA) in mm.

Conventional fractionation was used (66 Gy[RBE] in 33 fractions). Two robustly optimized IMPT plans were created for each patient with identical dosimetric goals using our inhouse developed TPS (10, 53). This in-house developed TPS had been fully validated and clinically commissioned for these two machines. We had successfully used this TPS to treat 5 complicated patients, including lung, head and neck, and central nervous system cancers, and regularly used it as secondary MU check for our commercial TPS. The number of spots and their respective positions prior to optimization varied since different proton machines were used. The number of spots for each case was included in Table 1 for both small-spot and large-spot machines. Logically, due to the smaller spot size, a larger number of spots were needed to cover the same targets.

Author Manuscript Author Manuscript Author Manuscript Author Manuscript

Robust Optimization

We modeled the random inter-fractional patient setup uncertainties by shifting the isocenter of the patient in the antero-posterior (A-P), superior-inferior (S-I), and right-left (R-L) directions by 5 mm, yielding 6 dose distributions and their corresponding influence matrices. Then we modeled systematic range uncertainties by scaling the stopping power ratios by ±3.5% (54, 55) and generated 2 dose distributions and influence matrices corresponding to minimum and maximum proton ranges, respectively.

Plans were generated on average 4D CTs with density overridden to IGTV (HU=50) (56), but the optimization target was set to be ITV. The impact of patient setup and range uncertainties was taken into account directly in the optimization algorithm rather than using margin expansion technique with the employment of planning target volume (PTV). The worst-case dose distribution was derived by choosing the smallest dose among the nine doses (8 perturbed dose distributions plus the nominal dose distribution) for each voxel in the ITV, along with the largest dose for each voxel outside the ITV. The resulting voxel-wise worst-case dose distribution was then used in robust optimization, which is different from the objective-wise and composite worst-case robust optimization methods discussed in Fredriksson and Bokrantz (57). The dose volume constraints used in the optimizations were included in Supplemental Table 1. All these objectives were included in the robust optimization.

The robustly optimized plan based on the large-spot machine was normalized to have the same ITV $D_{95\%}$ (the dose covering 95% of structure's volume) as the robustly optimized plan based on small-spot machine in the nominal scenario (without any uncertainties considered) for fair comparison. All plans were reviewed to ensure that they met institutional standards of the dose-volume constraints for targets and OARs (Supplemental Table 2).

Robustness Quantification

To evaluate and compare IMPT plans, we used a robustness quantification technique that displayed the envelope of all dose-volume histograms (DVHs) in band graphs of the 9 dose distributions associated with the corresponding range or setup uncertainties (10, 58). Please note that the plan robustness discussed here only included impact of setup and range uncertainties. The impact of motion will be discussed in the following subsection about interplay effects. We used the width of the DVH bands as a numerical index to evaluate the plan robustness: the smaller band width value indicated a more robust plan.

Dose Calculation with Interplay Effects

We developed software to calculate the dose under the influence of interplay effects (23, 49, 59, 60). The resulting dose was referred to as "dynamic dose" (61). In the software, time-dependent spot delivery parameters, 4D-CTs, and the time spent in each phase during the CT simulation were used to calculate the dose to a patient with interplay effects considered (the detailed spot delivery parameters are included in Table 2. The CTV defined at the exhale phase (CTV_{T50}) was used as the target and the dose was accumulated to the exhale phase. The minimum and maximum MU limits in small-spot machine setting were 0.003 and 0.04 MU respectively, while the minimum and maximum MU limits in large-spot machine setting

Author Manuscript Author Manuscript Author Manuscript Author Manuscript

were 0.005 and 0.04 MU, respectively. The same maximum MU limits were used for both machines. The iso-layer repainting technique used in this work is different from the iso-layer repainting technique (or the so-called “layered rescanning”) discussed in some previous literatures, for example, Grassberger et al.(39) and Li et al.(24). In our iso-layer repainting technique, a spot will be split into multiple spots of equal weights only if its intensity is larger than the maximum MU limit (0.04MU) (for example, a spot of 0.07MU will be split into two spots of 0.035MU and a spot of 0.081MU will be split into three spots of 0.027MU), and the split spots will be appended at the end of the spot list of the same energy layer and delivered through the iso-layer repainting. Otherwise no repainting will be performed for this spot (for example, a spot of 0.039MU). The energy ranges, numbers of energy layers, total repainting numbers and deliver durations in one fraction were different for different machines (Supplemental Table 3). We did not consider uncertainties in the dose calculation with interplay effects due to the increased computational burden.

We randomized the starting phase of each field per fraction to effectively model the impact of starting phase (49). For all patients, 5 runs with randomized starting phases were conducted for both plans to assess the influence of the randomized starting phases. The results of the DVH indices were presented using average values for the corresponding DVH indices (with all 5 runs) with error bars. The error bars indicated maximum and minimum values of the corresponding DVH indices as a result.

Plan Quality Evaluation

We calculated $D_{95\%}$, $D_{5\%}$ and D_{2cc} (the minimum dose for 2cc of the targets covered by the highest dose) from the ITV DVH. The ITV $D_{95\%}$ and $D_{5\%}$-$D_{95\%}$ were used to evaluate target dose coverage and homogeneity. The ITV was chosen as the target since it was routinely used in clinical practice. The dose covering a percentage of the structure’s volume ($D_{\%}$) was compared for various organs at-risk (OARs). Spinal cord D_{max}, esophagus $D_{33\%}$ and D_{mean}, total lung D_{mean}, heart $D_{33\%}$ and D_{mean} were used. In addition, relative volumes which received a dose at least a specific value such as total lung $V_{5Gy[RBE]}$ and $V_{20Gy[RBE]}$, esophagus $V_{60Gy[RBE]}$, and heart $V_{50Gy[RBE]}$, were also used.

Statistical Analysis

For a specific patient, the comparison of results between the two machines is patient specific. However, for a patient population, we have to use some statistical methods to reach statistically meaning conclusions. We used the two-tailed Wilcoxon signed rank test included in JMP Pro 10 software (SAS Institute Inc., Cary, North Carolina) to compare all paired metrics. *P*-values less than 0.05 were considered statistically significant. We also calculated the means of all metrics.

RESULTS

Plan quality

We compared plan quality in the nominal scenario (without any uncertainties considered). Compared to large-spot machine, small-spot machine created IMPT plans with comparable target dose coverage (unit: Gy[RBE]) [$D_{95\%}$ ITV: 65.21 vs. 65.25 (p=0.43); small-spot

Author Manuscript Author Manuscript Author Manuscript Author Manuscript

machine vs. large-spot machine], comparable target dose homogeneity [$D_{5\%}$-$D_{95\%}$ ITV: 3.73 vs. 3.77 (p=0.85)], comparable hot spots [D_{2cc} ITV: 73.97 vs. 75.52 (p=0.63)], and also comparable protection of most OARs [D_{max} spinal cord: 31.02 vs. 31.37 (p=0.08), D_{mean} total lung: 13.97 vs. 14.63 (p=0.16), $D_{33\%}$ esophagus: 34.73 vs. 35.53 (p=0.56), $V_{20Gy[RBE]}$ total lung: 25.43% vs. 26.64% (p=0.38), $V_{60Gy[RBE]}$ esophagus: 18.09% vs. 18.12% (p=0.70), and $V_{50Gy[RBE]}$ heart: 5.14% vs. 4.90% (p=0.65)] (Figure 1[c–d]). However, small-spot machine achieved significantly lower heart dose, esophagus D_{mean} and total lung $V_{5Gy[RBE]}$ [D_{mean} heart: 5.06 vs. 6.05 (p=0.002), $D_{33\%}$ heart: 0.28 vs. 1.72 (p=0.007), D_{mean} esophagus: 21.85 vs. 23.94 (p=0.02), and $V_{5Gy[RBE]}$ total lung: 33.40% vs. 37.24% (p=0.002)] (Figure 1[c–d]).

As an example, Figure 1(a) displays the dose distribution on an axial CT slice for patient 7, with results from large-spot machine on the *left* and small-spot machine on the *right*. This figure illustrates that robust optimization using small-spot machine considerably reduced the dose penumbra, and also rendered the dose distribution more conformal to the targets compared to robust optimization using large-spot machine. This considerably minimized the potential side effects to nearby OARs such as total lung and spinal cord for this patient.

Plan Robustness

For plan robustness (setup and range uncertainties) consideration, Figure 2(a–b) shows the means of DVH band widths of ITV and OARs for all 10 patients. p-values are displayed on the top of the columns. Figure 2(a) illustrated how we derived the ITV DVH band width at $D_{95\%}$ for one typical patient. Large-spot machine resulted in IMPT plans with plan robustness comparable to those of small-spot machine for ITV [$D_{95\%}$: 2.01 vs. 1.77 (p=0.23); $D_{5\%}$-$D_{95\%}$: 2.44 vs. 1.59 (p=0.13); D_{2cc}: 2.75 vs. 1.94 (p=0.23); small-spot machine vs. large-spot machine, units: Gy(RBE)], esophagus [$V_{60Gy[RBE]\%}$: 6.90% vs. 7.25% (p=0.63); $D_{33\%}$: 9.84 vs. 8.01 (p=0.32)], heart [D_{mean}: 2.51 vs. 2.61 (p=0.85); $V_{50Gy[RBE]}$: 2.85% vs. 2.84% (p=0.65)], total lung [D_{mean}: 1.88 vs. 1.76 (p=0.23); $V_{5Gy[RBE]}$: 4.49% vs. 4.18% (p=0.70); $V_{20Gy[RBE]}$: 3.53% vs. 3.29% (p=0.49)] and spinal cord [D_{max}: 14.10 vs. 12.14 (p=0.36)], while heart $D_{33\%}$ [0.70 vs. 1.85 (p=0.0039)] was statistically more robust for small-spot machine, and esophagus D_{mean} [5.39 vs. 4.49 (p=0.027)] was less robust for small-spot machine (Figure 2[b–c]).

Interplay Effects

With the interplay effects being considered, robust optimization with small-spot machine produced plans with comparable target coverage (Figure 3(a)) (unit: Gy[RBE]) [$D_{95\%}$ CTV_{T50}: 61.25 vs. 62.60 (p=0.23)], comparable target dose homogeneity [$D_{5\%}$-$D_{95\%}$ CTV_{T50}: 7.34 vs. 6.31 (p=0.19)], comparable target hot spots [D_{2cc} CTV_{T50}: 73.13 vs. 74.46 (p=0.16)], and comparable protection for most of the OARs [$V_{20Gy[RBE]}$ total lung: 25.13% vs. 26.24% (p=0.38), $D_{33\%}$ esophagus: 33.39 vs. 33.71 (p=0.77), D_{mean} total lung: 13.67 vs. 14.48 (p=0.11), $V_{60Gy[RBE]}$ esophagus: 16.52% vs. 16.81% (p=1.0), $V_{50Gy[RBE]}$ heart: 4.28% vs. 4.26% (p=0.67), D_{max} spinal cord: 37.34 vs. 38.46 (p=0.70)] (Figure 3(a–i)). However, small-spot machine performed significantly better in lowering heart dose, esophagus D_{mean}, and also total lung $V_{5Gy[RBE]}$ [D_{mean} heart: 4.65 vs. 5.59 (p=0.002), $D_{33\%}$

Author Manuscript Author Manuscript Author Manuscript Author Manuscript

heart: 0.22 vs. 1.53 (p=0.0039), D_{mean} esophagus: 21.04 vs. 22.92 (p=0.0274), $V_{5Gy[RBE]}$ total lung: 34.28% vs. 37.73% (p=0.0039)] (Figure 4(c–f)).

Figure 4(a–b) shows doses in the presence of interplay effects on an axial CT slice for patient 3, with results from large-spot machine (Figure 4(a)) and small-spot machine (Figure 4(b)). The same phenomenon as in Figure 1(a–b) was observed, i.e., robust optimization using small-spot machine considerably reduced the dose penumbra as compared with robust optimization using large-spot machine. This significantly improved the protection to the nearby OARs.

DISCUSSION

IMPT holds great promise for improving the treatment outcomes of lung cancer patient. However, the clinical effectiveness and quality of IMPT to treat lung cancer are dependent on plan robustness to uncertainties and interplay effects, especially for machines with small spots. Previously, plans with small spots were shown to be less robust (i.e., more susceptible) to motion effects than those with large spots (22). With interplay effects being considered, the target dose homogeneity was reduced with small-spot machines (the increase in $D_{5\%}$- $D_{95\%}$ due to interplay effects for large-spot machines was 5.6% ± 4.2% of the prescribed dose, compared to 15.8%± 11.1% for small-spot machines) (22). Similar results were observed by Dowdell et al. (21). Therefore, large-spot machines were generally believed to be more preferable than small-spot machines for treating lung cancer with IMPT (21, 22).

However, our results with robust optimization showed that given the same tumor coverage and prescription doses, small-spot machine may achieve significantly lower heart doses. The heart $D_{33\%}$ and mean dose are by average 505.9% and 19.6% smaller in the small-spot machine than the one in the large-spot machine. Heart dose has been found as an independent dosimetric predictor of overall survival in patients with locally advanced NSCLC (63, 64). Small-spot IMPT can also deliver significantly less doses to the esophagus and lungs. The total lung $V_{5Gy[RBE]}$, esophagus mean dose are by average 11.5% and 9.5% smaller in the small-spot machine than the one in the large-spot machine, which may reduce the risks of radiation esophagitis and pneumonitis for our patients treated by IMPT. These results are consistent with the report by Moteabbed et al. (65), however, their study did not consider plan robustness and interplay effects.

Furthermore, in the presence of uncertainties and with robust optimization considered, our results showed that small-spot machines can generate equally qualified and even more desirable IMPT plans as compared with large-spot machines. Additionally it is of potentially important significance that plans with small-spot machine also performed comparably or better in the treatment of lung cancer with interplay effects considered. Although different from the previous studies noted (21, 22), our results did strongly suggest that small-spot scanning proton beam machine may emerge as the preferred proton machine as treatment modality for lung cancer, and such effectiveness may also be extended to other disease sites including liver and esophagus (pending further studies). Our results support using the new generation of scanning proton beam machines with small spots to treat mobile tumors if the

Author Manuscript Author Manuscript Author Manuscript Author Manuscript

IMPT-related parameters are properly configured, and also there are reliable software tools and expertise in place to evaluate robustness and interplay effects.

Small-spot machines usually require smaller spot spacing to achieve sufficiently homogeneous dose distribution, especially in the direction orthogonal to the beam direction within the targets. In this study, large-spot machine had spot spacing of 6.5 mm to 20 mm, which is larger than the spot spacing (5 mm) used in the small-spot machine. Therefore a larger number of spots were required to cover the same target region using small-spot machines. From Table 1, an average of 3.13 (range: 1.15~9.82) times more spots were used for small-spot machine plans. A larger dimension of optimization variables gives the optimizer more freedom to compensate for higher sensitivity to uncertainties resulting from smaller spots in the presence of uncertainties (51).

In general, the number [mean (min~max)] of repainting among all energy layers used in the small-spot machine is smaller than or equal to the one used in the large-spot machine (Supplemental Table 3). This is because the MU per spot is usually smaller in the small-spot machine due to the much larger number of spots used in the small-spot machine compared to the large-spot machine. However, the field delivery duration for the small-spot machine is by average 28% longer than the one for the large-spot machine, which is mostly due to much more energy layers (38.4% more by average) used in the small-spot machine. The long field delivery time might result in more randomization and thus might mitigate the impact of interplay effects.(49, 66, 67)

It is also worthy to note that In Figure 3(a–c), we can see that patient 2 and 10 have the relatively large difference in CTV $D_{95\%}$ and patient 1 and patient 10 have relatively large difference in CTV $D_{5\%}$-$D_{95\%}$. We carefully checked the beam angles, breathing patterns, beam repainting patterns, motion amplitude, and tumor position and size etc. We did not find any characteristics of these patients significantly different from other patients. In order to reach statistically meaningful conclusions for the comparison between the two machines for a patient population, we have to use some statistical methods. These patients are the outliers in the study. On the other hand, as pointed out by several previous literatures (22, 25, 39, 49, 59, 65), the impact of interplay effects is patient-specific. Therefore the conclusions derived in this study might be only valid to the patients included in this study and it is highly recommended to perform the patient-specific evaluation of interplay effects for every patient in routine clinics (22, 25, 39, 49, 59, 65).

This study has several limitations. First, patients received 4D simulation CT, but no attempt was made to do motion-based adaptation to the treatment plans. The patient's respiratory patterns in the treatment most likely were different from those during simulation and may vary from day to day. Fortunately, the day-to-day difference in breathing motion usually leads to less distorted dose distributions due to the averaging effect on the dose distribution (15). Second, the robustness quantification considered only nine uncertainty scenarios. In reality, patient setup uncertainty, proton beam range uncertainty, body deformation, inter-field motion, and rotational uncertainty can co-exist and influence one another simultaneously. Therefore, the robustness quantification could underestimate or overestimate the impact of these additional uncertainties (68). Third and finally, there are other techniques

Author Manuscript Author Manuscript Author Manuscript Author Manuscript

used to reduce the impact of interplay effects, such as gating, repainting, breath holding, tumor tracking, and range-adapted ITV; further evaluation of these various different techniques on plans with small-spot machine are also urgently needed.

Conclusion

Robust optimization with small-spot machines significantly improves heart, lung, and esophagus sparing with similar target coverage, plan robustness and interplay effects compared to plans generated by traditional large-spot machines. This study demonstrated the potential benefits and feasibility for using small-spot machine in IMPT to treat lung cancer patients in the future.

Supplementary Material

Refer to Web version on PubMed Central for supplementary material.

Acknowledgments

This research was supported by the National Cancer Institute (NCI) Career Developmental Award K25CA168984, by Arizona Biomedical Research Commission Investigator Award, by the Fraternal Order of Eagles Cancer Research Fund Career Development Award, by The Lawrence W. and Marilyn W. Matteson Fund for Cancer Research, by Mayo Arizona State University Seed Grant, and by The Kemper Marley Foundation.

References

1. Siegel RL, Miller KD, Jemal A. Cancer statistics, 2016. CA: a cancer journal for clinicians. 2016; 66:7–30. [PubMed: 26742998]
2. Register SP, Zhang X, Mohan R, et al. Proton stereotactic body radiation therapy for clinically challenging cases of centrally and superiorly located stage I non-small-cell lung cancer. International Journal of Radiation Oncology*Biology*Physics. 2011; 80:1015–1022.
3. Stuschke M, Kaiser A, Pottgen C, et al. Potentials of robust intensity modulated scanning proton plans for locally advanced lung cancer in comparison to intensity modulated photon plans. Radiotherapy and oncology : journal of the European Society for Therapeutic Radiology and Oncology. 2012; 104:45–51. [PubMed: 22560714]
4. Zhang X, Li Y, Pan X, et al. Intensity-modulated proton therapy reduces the dose to normal tissue compared with intensity-modulated radiation therapy or passive scattering proton therapy and enables individualized radical radiotherapy for extensive stage IIIB non-small-cell lung cancer: a virtual clinical study. Int J Radiat Oncol Biol Phys. 2010; 77
5. Lomax, AJ. Department of Physics. Vol PhD. Zurich: ETH; 2004. Intensity modulated proton therapy: the potential and the challenge.
6. Lomax AJ. Intensity modulated proton therapy and its sensitivity to treatment uncertainties 2: the potential effects of inter-fraction and inter-field motions. Physics in Medicine and Biology. 2008; 53:1043–1056. [PubMed: 18263957]
7. Chen W, Unkelbach J, Trofimov A, et al. Including robustness in multi-criteria optimization for intensity-modulated proton therapy. Physics in Medicine and Biology. 2012; 57:591–608. [PubMed: 22222720]
8. Fredriksson A, Forsgren A, Hardemark B. Minimax optimization for handling range and setup uncertainties in proton therapy. Medical Physics. 2011; 38:1672–1684. [PubMed: 21520880]
9. Liu W, Li Y, Li X, et al. Influence of robust optimization in intensity-modulated proton therapy with different dose delivery techniques. Med. Phys. 2012; 39:3089–4001. [PubMed: 22755694]
10. Liu W, Zhang X, Li Y, et al. Robust optimization in intensity-modulated proton therapy. Med. Phys. 2012; 39:1079–1091. [PubMed: 22320818]

Author Manuscript Author Manuscript Author Manuscript Author Manuscript

11. Pflugfelder D, Wilkens JJ, Oelfke U. Worst case optimization: a method to account for uncertainties in the optimization of intensity modulated proton therapy. Physics in Medicine and Biology. 2008; 53:1689–1700. [PubMed: 18367797]
12. Unkelbach J, Bortfeld T, Martin BC, et al. Reducing the sensitivity of IMPT treatment plans to setup errors and range uncertainties via probabilistic treatment planning. Medical Physics. 2009; 36:149–163. [PubMed: 19235384]
13. Unkelbach J, Chan TCY, Bortfeld T. Accounting for range uncertainties in the optimization of intensity modulated proton therapy. Physics in Medicine and Biology. 2007; 52:2755–2773. [PubMed: 17473350]
14. Liu W, Liao Z, Schild SE, et al. Impact of respiratory motion on worst-case scenario optimized intensity modulated proton therapy for lung cancers. Practical Radiation Oncology. 2015; 5:e77–86. [PubMed: 25413400]
15. Kraus KM, Heath E, Oelfke U. Dosimetric consequences of tumor motion due to respiration for a scanned proton beam. Phys. Med. Biol. 2011; 56:6563–6581. [PubMed: 21937770]
16. Phillips MH, Pedroni E, Blattmann H, et al. EFFECTS OF RESPIRATORY MOTION ON DOSE UNIFORMITY WITH A CHARGED-PARTICLE SCANNING METHOD. Physics in Medicine and Biology. 1992; 37:223–234. [PubMed: 1311106]
17. Lambert J, Suchowerska N, McKenzie DR, et al. Intrafractional motion during proton beam scanning. Physics in Medicine and Biology. 2005; 50:4853–4862. [PubMed: 16204877]
18. Grozinger SO, Bert C, Haberer T, et al. Motion compensation with a scanned ion beam: a technical feasibility study. Radiation Oncology. 2008; 3
19. Seco J, Robertson D, Trofimov A, et al. Breathing interplay effects during proton beam scanning: simulation and statistical analysis. Physics in Medicine and Biology. 2009; 54:N283–N294. [PubMed: 19550002]
20. Grozinger SO, Rietzel E, Li Q, et al. Simulations to design an online motion compensation system for scanned particle beams. Physics in Medicine and Biology. 2006; 51:3517–3531. [PubMed: 16825746]
21. Dowdell S, Grassberger C, Sharp GC, et al. Interplay effects in proton scanning for lung: a 4D Monte Carlo study assessing the impact of tumor and beam delivery parameters. Physics in Medicine and Biology. 2013; 58:4137–4156. [PubMed: 23689035]
22. Grassberger C, Dowdell S, Lomax A, et al. Motion Interplay as a Function of Patient Parameters and Spot Size in Spot Scanning Proton Therapy for Lung Cancer. International Journal of Radiation Oncology Biology Physics. 2013; 86:380–386.
23. Knopf A-C, Hong TS, Lomax A. Scanned proton radiotherapy for mobile targets-the effectiveness of re-scanning in the context of different treatment planning approaches and for different motion characteristics. Physics in Medicine and Biology. 2011; 56:7257–7271. [PubMed: 22037710]
24. Li Y, Kardar L, Li X, et al. On the interplay effects with proton scanning beams in stage III lung cancer. Medical Physics. 2014; 41
25. Kardar L, Li Y, Li X, et al. Evaluation and mitigation of the interplay effects of intensity modulated proton therapy for lung cancer in a clinical setting. Practical Radiation Oncology. 2014; 4:e259–268. [PubMed: 25407877]
26. Bortfeld T, Jokivarsi K, Goitein M, et al. Effects of intra-fraction motion on IMRT dose delivery: statistical analysis and simulation. Physics in Medicine and Biology. 2002; 47:2203–2220. [PubMed: 12164582]
27. Knopf A-C, Boye D, Lomax A, et al. Adequate margin definition for scanned particle therapy in the incidence of intrafractional motion. Physics in Medicine and Biology. 2013; 58:6079–6094. [PubMed: 23939146]
28. Rietzel E, Bert C. Respiratory motion management in particle therapy. Medical Physics. 2010; 37:449–460. [PubMed: 20229853]
29. Graeff C, Durante M, Bert C. Motion mitigation in intensity modulated particle therapy by internal target volumes covering range changes. Medical Physics. 2012; 39:6004–6013. [PubMed: 23039638]

Author Manuscript Author Manuscript Author Manuscript Author Manuscript

30. Dueck J, Knopf AC, Lomax A, et al. Robustness of the Voluntary Breath-Hold Approach for the Treatment of Peripheral Lung Tumors Using Hypofractionated Pencil Beam Scanning Proton Therapy. Int J Radiat Oncol Biol Phys. 2016; 95:534–541. [PubMed: 26797540]
31. Matsuura T, Miyamoto N, Shimizu S, et al. Integration of a real-time tumor monitoring system into gated proton spot-scanning beam therapy: an initial phantom study using patient tumor trajectory data. Med Phys. 2013; 40:071729. [PubMed: 23822433]
32. Shimizu S, Matsuura T, Umezawa M, et al. Preliminary analysis for integration of spot-scanning proton beam therapy and real-time imaging and gating. Phys Med. 2014; 30:555–558. [PubMed: 24786663]
33. Shimizu S, Miyamoto N, Matsuura T, et al. A proton beam therapy system dedicated to spot-scanning increases accuracy with moving tumors by real-time imaging and gating and reduces equipment size. PLoS One. 2014; 9:e94971. [PubMed: 24747601]
34. Rietzel E, Bert C. Respiratory motion management in particle therapy. Med Phys. 2010; 37:449–460. [PubMed: 20229853]
35. Knopf A, Bert C, Heath E, et al. Special report: workshop on 4D-treatment planning in actively scanned particle therapy--recommendations, technical challenges, and future research directions. Med Phys. 2010; 37:4608–4614. [PubMed: 20964178]
36. Grassberger C, Dowdell S, Lomax A, et al. Motion interplay as a function of patient parameters and spot size in spot scanning proton therapy for lung cancer. Int J Radiat Oncol Biol Phys. 2013; 86:380–386. [PubMed: 23462423]
37. Bernatowicz K, Lomax AJ, Knopf A. Comparative study of layered and volumetric rescanning for different scanning speeds of proton beam in liver patients. Phys Med Biol. 2013; 58:7905–7920. [PubMed: 24165090]
38. Schatti A, Zakova M, Meer D, et al. Experimental verification of motion mitigation of discrete proton spot scanning by re-scanning. Phys Med Biol. 2013; 58:8555–8572. [PubMed: 24254249]
39. Grassberger C, Dowdell S, Sharp G, et al. Motion mitigation for lung cancer patients treated with active scanning proton therapy. Med Phys. 2015; 42:2462–2469. [PubMed: 25979039]
40. Kardar L, Li Y, Li X, et al. Evaluation and mitigation of the interplay effects of intensity modulated proton therapy for lung cancer in a clinical setting. Pract Radiat Oncol. 2014; 4:e259–268. [PubMed: 25407877]
41. Zenklusen SM, Pedroni E, Meer D. A study on repainting strategies for treating moderately moving targets with proton pencil beam scanning at the new Gantry 2 at PSI. Phys Med Biol. 2010; 55:5103–5121. [PubMed: 20702927]
42. Zhang Y, Knopf AC, Weber DC, et al. Improving 4D plan quality for PBS-based liver tumour treatments by combining online image guided beam gating with rescanning. Phys Med Biol. 2015; 60:8141–8159. [PubMed: 26439493]
43. Phillips MH, Pedroni E, Blattmann H, et al. Effects of respiratory motion on dose uniformity with a charged particle scanning method. Phys Med Biol. 1992; 37:223–234. [PubMed: 1311106]
44. Knopf AC, Hong TS, Lomax A. Scanned proton radiotherapy for mobile targets-the effectiveness of re-scanning in the context of different treatment planning approaches and for different motion characteristics. Phys Med Biol. 2011; 56:7257–7271. [PubMed: 22037710]
45. Eley JG, Newhauser WD, Richter D, et al. Robustness of target dose coverage to motion uncertainties for scanned carbon ion beam tracking therapy of moving tumors. Physics in Medicine and Biology. 2015; 60:1717–1740. [PubMed: 25650520]
46. Graeff C. Motion mitigation in scanned ion beam therapy through 4D-optimization. Physica Medica-European Journal of Medical Physics. 2014; 30:570–577.
47. Graeff C, Constantinescu A, Luechtenborg R, et al. Multigating, a 4D Optimized Beam Tracking in Scanned Ion Beam Therapy. Technology in Cancer Research & Treatment. 2014; 13:497–504. [PubMed: 24354752]
48. Graeff C, Luechtenborg R, Eley JG, et al. A 4D-optimization concept for scanned ion beam therapy. Radiotherapy and Oncology. 2013; 109:419–424. [PubMed: 24183865]
49. Liu W, Schild SE, Chang JY, et al. Exploratory Study of 4D versus 3D Robust Optimization in Intensity Modulated Proton Therapy for Lung Cancer. International Journal of Radiation Oncology Biology Physics. 2016; 95:523–533.

Author Manuscript Author Manuscript Author Manuscript Author Manuscript

50. Inoue T, Widder J, van Dijk LV, et al. Limited Impact of Setup and Range Uncertainties, Breathing Motion, and Interplay Effects in Robustly Optimized Intensity Modulated Proton Therapy for Stage III Non-small Cell Lung Cancer. Int J Radiat Oncol Biol Phys. 2016; 96:661–669. [PubMed: 27681763]
51. Sio TT, Merrell KW, Beltran CJ, et al. Spot-scanned pancreatic stereotactic body proton therapy: A dosimetric feasibility and robustness study. Physica Medica-European Journal of Medical Physics. 2016; 32:331–342.
52. Zhu XR, Sahoo N, Zhang X, et al. Intensity modulated proton therapy treatment planning using single-field optimization: The impact of monitor unit constraints on plan quality. Medical Physics. 2010; 37:1210–1219. [PubMed: 20384258]
53. Liu W, Li Y, Li X, et al. Influence of robust optimization in intensity-modulated proton therapy with different dose delivery techniques. Med Phys. 2012; 39
54. Moyers MF, Miller DW, Bush DA, et al. Methodologies and tools for proton beam design for lung tumors. Int J Radiat Oncol Biol Phys. 2001; 49:1429–1438. [PubMed: 11286851]
55. Yang M, Zhu XR, Park PC, et al. Comprehensive analysis of proton range uncertainties related to patient stopping-power-ratio estimation using the stoichiometric calibration. Physics in Medicine and Biology. 2012; 57:4095–4115. [PubMed: 22678123]
56. Kang Y, Zhang X, Chang JY, et al. 4D proton treatment planning strategy for mobile lung tumors. International Journal of Radiation Oncology Biology Physics. 2007; 67:906–914.
57. Fredriksson A, Bokrantz R. A critical evaluation of worst case optimization methods for robust intensity-modulated proton therapy planning. Medical Physics. 2014; 41:48–58.
58. Trofimov A, Kang J, Unkelbach J, et al. Evaluation of dosimetric gain and uncertainties in proton therapy delivery with scanned pencil beam in treatment of base-of-skull and spinal Tumors. International Journal of Radiation Oncology Biology Physics. 2010; 78:S133–S134.
59. Li Y, Zhang X, Li X, et al. Evaluating 4D interplay effects for proton scanning beams in lung cancers. Med. Phys. 2009; 36:2759.
60. Richter D, Schwarzkopf A, Trautmann J, et al. Upgrade and benchmarking of a 4D treatment planning system for scanned ion beam therapy. Medical Physics. 2013; 40
61. Li H, Li Y, Zhang X, et al. Dynamically accumulated dose and 4D accumulated dose for moving tumors. Medical Physics. 2012; 39:7359–7367. [PubMed: 23231285]
62. Shen J, Tryggestad E, Younkin JE, et al. Using experimentally determined proton spot scanning timing parameters to accurately model beam delivery time. Medical Physics. 2017
63. Speirs CK, DeWees TA, Rehman S, et al. Heart Dose Is an Independent Dosimetric Predictor of Overall Survival in Locally Advanced Non–Small Cell Lung Cancer. Journal of Thoracic Oncology. 2017; 12:293–301. [PubMed: 27743888]
64. Darby SC, Ewertz M, McGale P, et al. Risk of Ischemic Heart Disease in Women after Radiotherapy for Breast Cancer. New England Journal of Medicine. 2013; 368:987–998. [PubMed: 23484825]
65. Moteabbed M, Yock TI, Depauw N, et al. Impact of Spot Size and Beam-Shaping Devices on the Treatment Plan Quality for Pencil Beam Scanning Proton Therapy. International Journal of Radiation Oncology Biology Physics. 2016; 95:190–198.
66. Bert C, Grozinger SO, Rietzel E. Quantification of interplay effects of scanned particle beams and moving targets. Physics in Medicine and Biology. 2008; 53:2253–2265. [PubMed: 18401063]
67. Knopf AC, Hong TS, Lomax A. Scanned proton radiotherapy for mobile targets-the effectiveness of re-scanning in the context of different treatment planning approaches and for different motion characteristics. Physics in Medicine and Biology. 2011; 56:7257–7271. [PubMed: 22037710]
68. Quan M, Liu W, Wu R, et al. Preliminary evaluation of multi-field and single-field optimization for the treatment planning of spot-scanning proton therapy of head and neck cancer. Med. Phys. 2013; 40:081709. [PubMed: 23927306]

Author Manuscript Author Manuscript Author Manuscript Author Manuscript

Summary

We investigated how spot size and spacing affect plan quality, robustness and interplay effects of robustly-optimized IMPT for lung cancer. We found that compared to large-spot machine, small-spot machine significantly improved heart and esophagus sparing with comparable plan robustness and interplay effects. Small-spot machine requires more spots to cover the same tumor volume, which gives the optimizer more freedom to compensate for the higher sensitivity to uncertainties and interplay effects for lung cancer treatment.

Author Manuscript
Author Manuscript
Author Manuscript
Author Manuscript

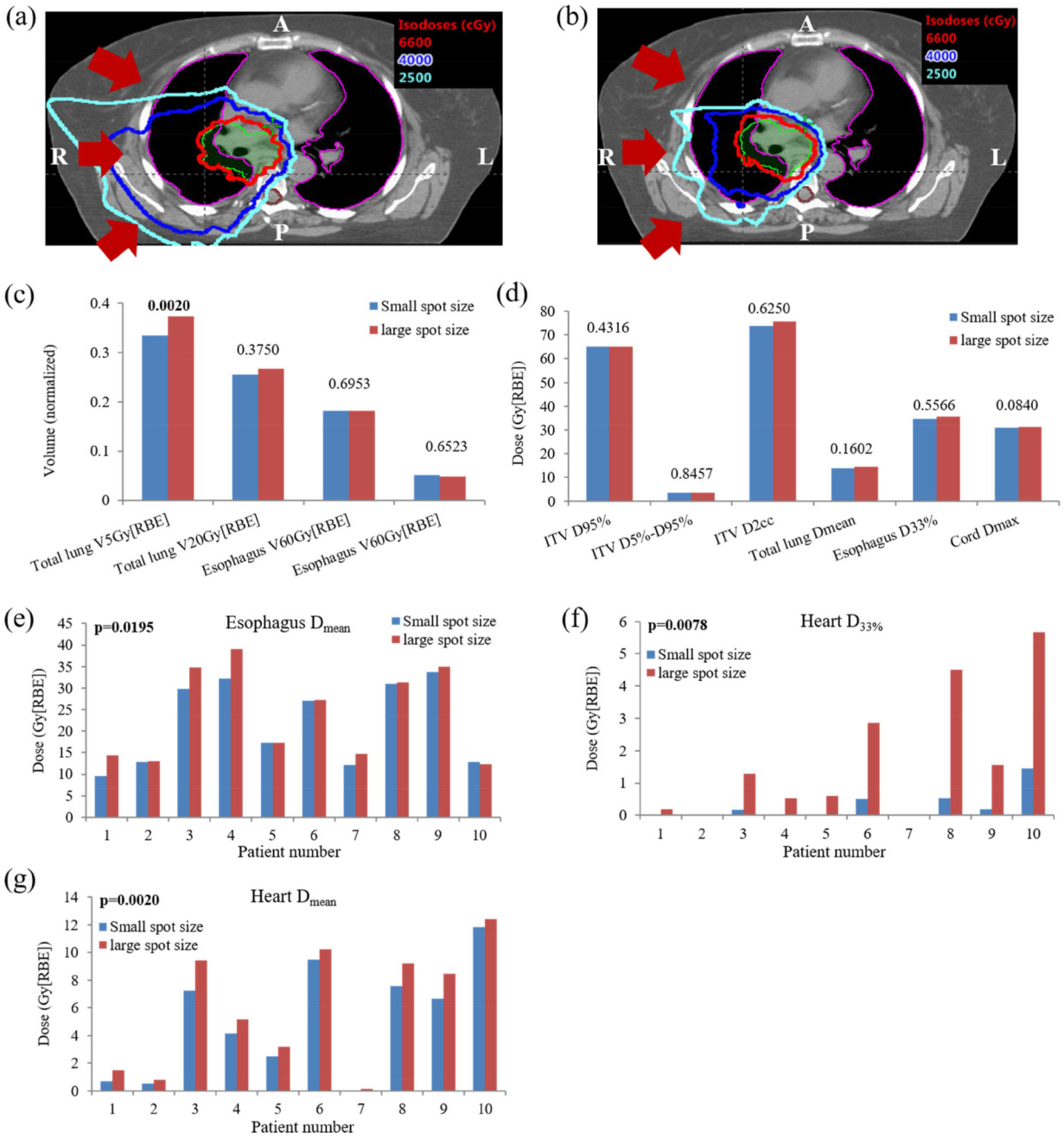

Figure 1.

Comparison of nominal dose distributions and DVH indices from large-spot and small-spot machines. A representative dose distribution comparison on one CT slice between (a) using large-spot and (b) using small-spot machine illustrated that small-spot machine decreased dose to total lung and spinal cord. The red arrows indicate beam directions. Comparison of the averaged DVH indices of different structures for ten lung cancer cases including (c) total lung $V_{5Gy[RBE]}$ and $V_{20Gy[RBE]}$, esophagus $V_{60Gy[RBE]}$, heart $V_{50Gy[RBE]}$, (d) ITV $D_{95\%}$, $D_{5\%}$- $D_{95\%}$, D_{2cc}, total lung D_{mean}, esophagus $D_{33\%}$, and spinal cord D_{max}, Comparison of nominal plan quality for 10 patients including: (e) esophagus D_{mean}, (f) heart $D_{33\%}$, and (g)

heart D_{mean}. Numbers at the top of the columns in (c) and (d) were *p* values from Wilcoxon signed-rank test. The indices with significant difference were labeled with the bold font.
Abbreviations: RBE = relative biological effectiveness.

Author Manuscript Author Manuscript Author Manuscript Author Manuscript

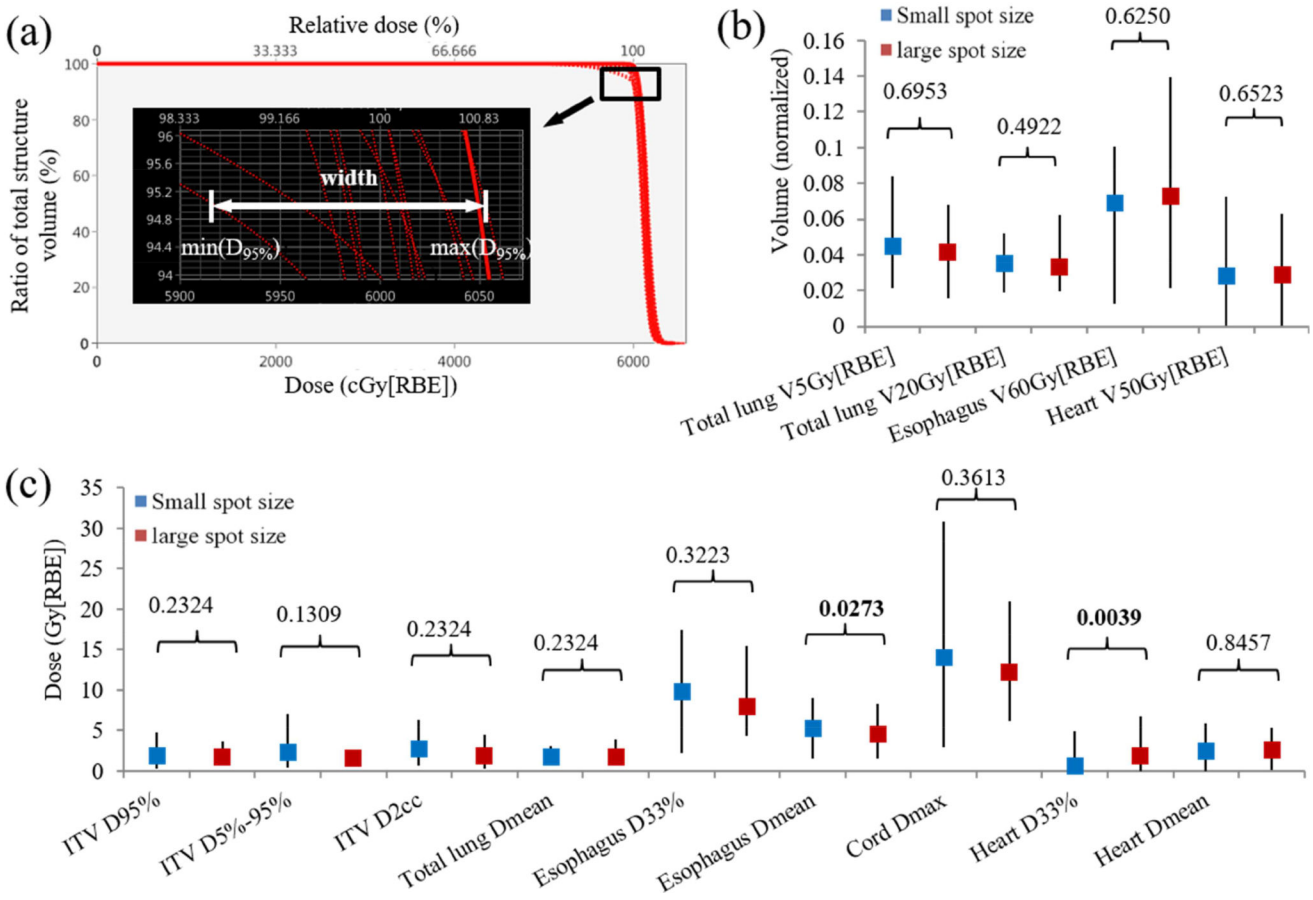

Figure 2.

Plan robustness evaluation using the DVH band method including (a) illustration of how we derived the ITV DVH band width at $D_{95\%}$ for one typical patient. (b) Averaged DVH band width for total lung $V_{5Gy[RBE]}$ and $V_{20Gy[RBE]}$, esophagus $V_{60Gy[RBE]}$, heart $V_{50Gy[RBE]}$, and (c) averaged DVH band width for ITV $D_{95\%}$, $D_{5\%}$- $D_{95\%}$, and D_{2cc}, total lung D_{mean}, esophagus $D_{33\%}$ and D_{mean}, spinal cord D_{max}, heart $D_{33\%}$ and D_{mean}, respectively. Numbers at the top of the columns in (b) and (c) were p values from Wilcoxon signed-rank test. The error bars in (b) and (c) showed the maximum and minimum values among the 10 patients. Abbreviations: RBE = relative biological effectiveness.

Author Manuscript Author Manuscript Author Manuscript Author Manuscript

Author Manuscript Author Manuscript Author Manuscript Author Manuscript

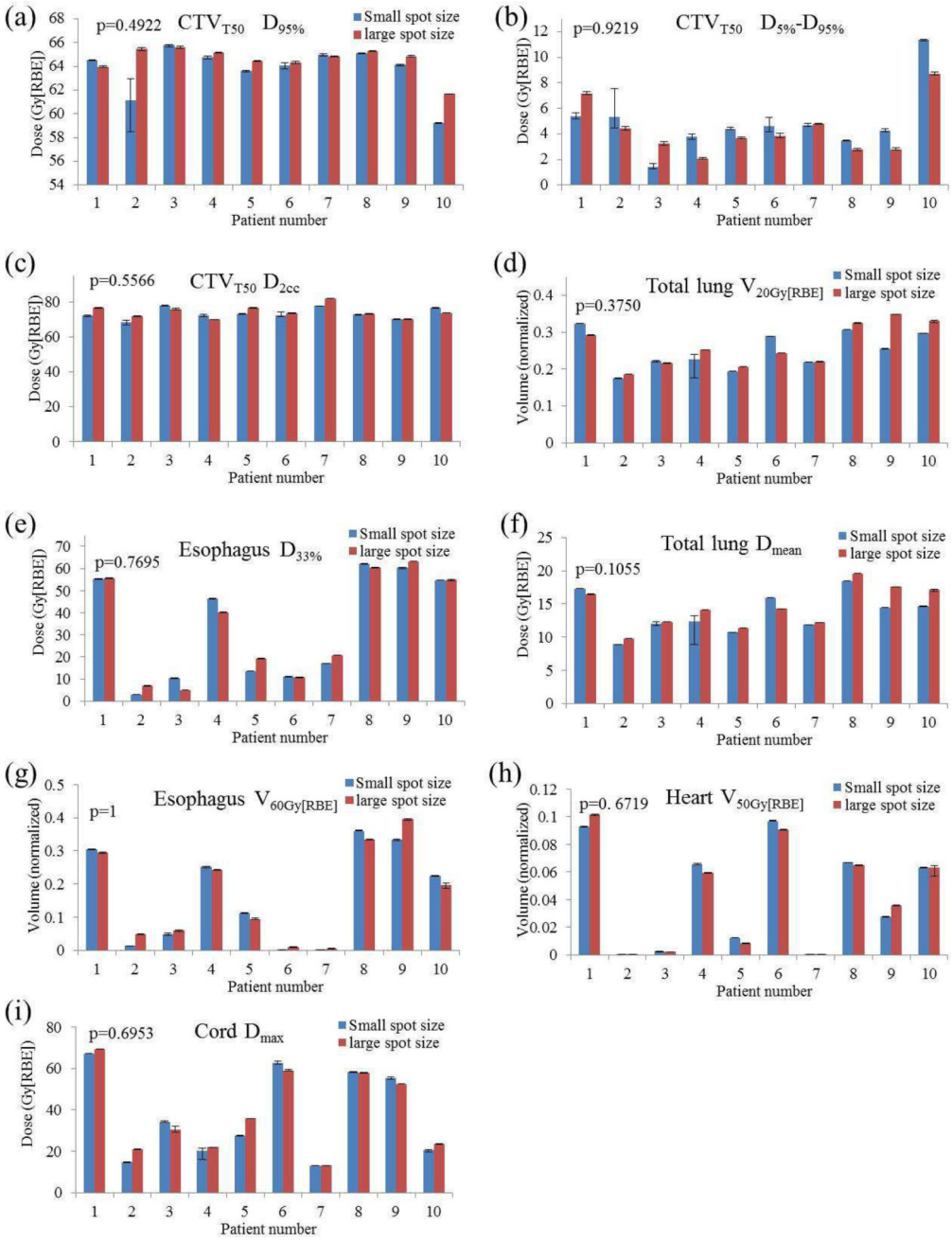

Figure 3.

Comparison of interplay effects for 10 patients including (a) CTV_{T50} $D_{95\%}$, (b) CTV_{T50} $D_{5\%}$- $D_{95\%}$, (c) CTV_{T50} D_{2cc}, (d) total lung $V_{20Gy[RBE]}$, (e) esophagus $D_{33\%}$, (f) total lung D_{mean}, (g) esophagus $V_{60Gy[RBE]}$, (h) heart $V_{50Gy[RBE]}$, and (i) spinal cord D_{max}. Averaged values from all 5 runs were shown. Error bars indicate the minimum and maximum values calculated from all 5 runs. P values at the top-left of the bar-plots were calculated using Wilcoxon signed-rank test. *Abbreviations:* RBE = relative biological effectiveness.

Author Manuscript Author Manuscript Author Manuscript Author Manuscript

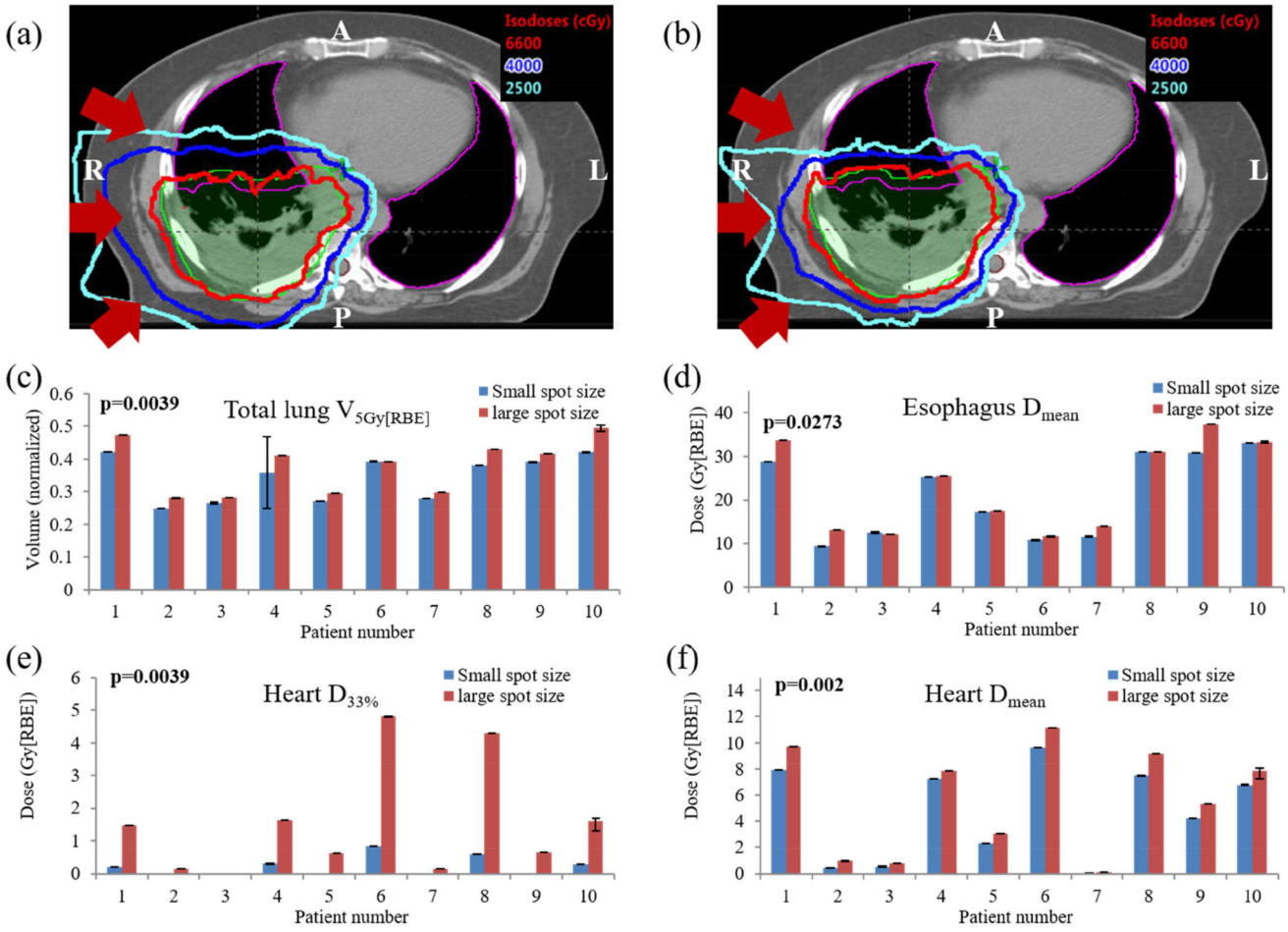

Figure 4.

Comparison of dose distributions with interplay effects at individual CT slice level illustrates that plans using large-spot machine (a) delivered higher dose to nearby healthy organs than the plan using (b) small-spot machine. There was statistically significant difference in (c) total lung $V_{5Gy[RBE]}$, (d) esophagus D_{mean}, (e) heart $D_{33\%}$, and (f) heart D_{mean}, illustrating plans using small-spot machine protected the lung, esophagus and heart better than large-spot machine. Averaged values from all 5 runs are shown. (c~f) Error bars indicate the minimum and maximum values among 5 runs. P values were calculated by Wilcoxon signed-rank testing. *Abbreviations:* RBE = relative biological effectiveness.

Author Manuscript Author Manuscript Author Manuscript Author Manuscript

Table 1

Tumor location, stage, ITV volume, respiratory motion amplitude (RMA), and number of spots with small spot and large spot

Patient	Tumor Location	Tumor Stage	ITV Volume (cm^3)	RMA (mm)	# Spots to cover the targets	
					Small Spots	Large Spots
1	Right upper	III	124.3	4.9	12,224	4,359
2	Right upper	II	251.3	8.2	18,438	4,148
3	Right upper	III	623.6	4.0	39,409	12,613
4	Right lower	III	825.4	15.0	51,370	44,576
5	Left lower	III	724.9	8.5	42,954	22,722
6	Right middle	III	373.5	13.0	26,164	10,849
7	Right upper	III	531.0	2.0	30,697	13,425
8	Right middle	III	1314.0	3.0	53,854	36,021
9	Right upper	IV	492.7	3.5	40,709	25,367
10	Left upper	III	575.4	5.0	42,305	4,308

ITV: internal target volume; RMA: respiratory motion amplitude;

#: Number of

Int J Radiat Oncol Biol Phys. Author manuscript; available in PMC 2019 June 01.

Author Manuscript

Author Manuscript

Author Manuscript

Author Manuscript

Table 2

Comparison of two machine characteristics(62)

	Large-spot Machine	Small-spot Machine
Spot Size (In-air at Isocenter)	Energy-dependent (σ: 5–15 mm)	Energy-dependent (σ: 2–6 mm)
Spot Spacing	Energy-dependent (1.3σ)	Fixed (5 mm)
Minimal MU Limit (MU)	0.005	0.003
Maximum MU Limit (MU)	0.04	0.04
Energy Layer Switching Time (s)	1.9	
Spill Length (s)	7.9	
Effective Magnet Scanning Speed in Horizontal Direction, V_x (m/s)	Medium Energy Group: 5.7	
	Low Energy Group: 7.0	
Effective Magnet Scanning Speed in Vertical Direction, V_y (m/s)	High Energy Group: 17.1	
	Medium Energy Group: 18.2	
	Low Energy Group: 22.2	
Magnet Preparation/Verification Time (ms)	1.93	
Proton Spill Rate (MU/s)	High Energy Group: 9.8	
	Medium Energy Group: 8.1	
	Low Energy Group: 8.5	

MU: Monitor Unit